

Multi-Objective Optimization of Micro-Channel Heat Sink For Liquid-Cooled Microelectronics

Iman Gholaminezhad
Graduate student
School of mechanical engineering
Shiraz University
Shiraz, Iran
Email:
Iman.gholaminezhad@shirazu.ac.ir

Hirad Assimi
Graduate student
Department of mechanical engineering
University of Guilan
Rasht, Iran
Email:
assimi@msc.guilan.ac.ir

Ali Jamali
Associate Professor
Department of mechanical engineering
University of Guilan
Rasht, Iran
Email:
ali.jamali@guilan.ac.ir

Abstract— More compact electronic circuits demand efficient methods to dissipate high generated heat flux. Micro channel heat sinks are efficient solution for cooling problem by a liquid coolant. In this paper, a multi-objective design procedure employed to optimize the cooling performance and energy management of a rectangular single-phase micro-channel heat sink. The design variables include geometric parameters that affect the micro-channel performance and objective functions include thermal resistance and pressure drop along microchannel. The optimum point showed lower energy consumption and higher cooling performance with considering lower mass flow rate of coolant in contrast with previous studies. Finally, an uncertainty quantification methodology based on Monte Carlo Simulations is also applied to study the effect of uncertain input parameters to the output quantities of interest. The statistical results show that the suggested geometry is reliable for real world applications for uncertainty range of 3-7% in design variables.

Keywords—component; Uncertainty quantification; heat sink; multi-objective; micro-channel; microelectronics

NOMENCLATURE

A_{hs}	Foot print of microchannel heat sink (m^2)
A_s	Foot print of heat source (m^2)
Cp_f	Specific heat of coolant [$J/(Kg.K)$]
D_h	Hydraulic diameter of microchannel (m)
f	Friction factor
K	Pressure loss coefficient
k_f	Thermal conductivity of coolant [$W/(m.K)$]
k_{hs}	Thermal conductivity of heat sink [$W/(m.K)$]
\dot{m}	Total mass flow rate of coolant through channels
Nu	Nusselt number
ΔP	Pressure drop (Pa)
Q	Total heat (W)
R_{th}	Thermal resistance ($^{\circ}C/W$)
T_{hs-max}	Maximum temperature of heat sink ($^{\circ}C$)
T_{f-in}	Inlet temperature of coolant ($^{\circ}C$)
u_m	Average flow velocity (m/s)

V_f	Volumetric flow rate of coolant through channels (m^3/s)
W_s	Width of heat source (m)
μ_f	Viscosity of coolant [$kg/(m.s)$]
ρ_f	Density of coolant (kg/m^3)

I. INTRODUCTION

Nowadays, both researchers and practitioners try to dwindle electronic components -such as electronic chips, semiconductors and etc. This endeavor leads to building ever more compact electronic circuits. Micro-electro-mechanical systems (MEMS) are propitious in electronic industry which these devices are expected to be used widely in future [1]. These developments require efficient methods to dissipate the heat flux from electronic components. It's proved that the electronic device or the electronic circuit temperatures can affect the performance of electronic devices [2]. Forced air convection can be a potential solution but it's only appropriate for the large-scale integration. Recently, many studies have been conducted and proposed Micro-channel heat sinks as efficient solution to this issue [3, 4]. Micro-channel heat sinks benefit from having a high ratio of surface area to volume, compactness and lightweight [5].

Generally, design and optimization of micro-channel heat sinks can be approached in two ways. The first and the more widespread one uses numerical simulations (such as computational fluid dynamics) for dealing with the problem however, the latter approach uses analytical and empirical formulations.

Optimization of the ultimate design plays an important role and is an inevitable step in engineering design problems. Evolutionary algorithms are prominent methods to solve the optimization problem as a direct method in contrast with conventional methods such as gradient based methods. Differential evolution is a powerful evolutionary algorithm which introduced by Storn and Price in 1997 [6].

Uncertainty quantification is the science of quantitative characterization which determines the effect of input uncertainties on the output quantities of interest.

There are commonly two types of uncertainties: aleatory and epistemic [7, 8]. Aleatory uncertainties are associated with physical variability in the system and environment which are

typically handled using probabilistic methods. Examples are: material properties, operating condition manufacturing, tolerance, etc. Epistemic uncertainties are referring to those that are due to the lack of knowledge, such as turbulent model assumptions. They can be reduced by increasing our knowledge of the system for example by performing more experiments. In this study, we have just considered aleatoric uncertainty.

In order to analyze the uncertainty of a system, statistical methods should be employed. Monte Carlo Simulations is a direct and simple numerical method for uncertainty quantification. It generates random samples considering predefined probabilistic distributions for uncertain parameters.

In this study, we used a multi-objective optimization kind of the differential evolution algorithm [9] to solve the problem. The geometric parameters of the microchannel heat sink are optimized by minimization of the two considered objective functions namely, total thermal resistance and pressure drop along the microchannels. Subsequently, we performed an uncertainty quantification procedure based on Monte Carlo Simulations. The statistical performance of the system is shown based on probability density function (PDF) and cumulative distribution function (CDF) of objective functions. Such probabilistic analysis helps the designer to find the input variables to which the objective functions are most sensitive, and thereby use the information for better design of experiments based on the most sensitive input parameters.

II. MATHEMATICAL MODEL

Fig. 1 shows the geometrical schematic of microchannel heatsink. The coolant is considered as water, single-phase and laminar which is fully developed for microfluidic applications. The radiation and free convection from microchannel external surface are neglected due to comparison with forced convection along the microchannels.

Equation (1) presents total thermal resistance relation which includes fin resistance (R_{fin}), capacitive resistance (R_{cap}), conductive resistance (R_{con}) and spreading resistance (R_{sp}).

$$R_{tot} = \frac{T_{hs-max} - T_{f-in}}{Q} = R_{fin} + R_{cap} + R_{con} + R_{sp} \quad (1)$$

Equations (2-5) define conductive, capacitive, fin and spreading thermal resistances, respectively.

$$R_{con} = \frac{t}{K_{hs} A_{hs}} \quad (2)$$

$$R_{cap} = \frac{1}{\dot{m} C_{p_f}} = \frac{1}{2 \rho_f C_{p_f} V_f} = \frac{1}{C_{p_f} \mu_f Re} \frac{1 + \beta}{1 + \alpha} \frac{L_{hs}}{A_{hs}} \quad (3)$$

$$R_{fin} = \frac{1}{Nu} \frac{1}{K_f} \frac{1 + \beta}{1 + 2\alpha\eta} \frac{2\alpha}{1 + \alpha} \frac{W_{ch}}{A_{hs}} \quad (4)$$

$$R_{sp} = \frac{2}{k_{hs} W_{hs} L_{hs} W_s^2} \sum_{i=1}^{\infty} A_i \frac{\cos(\lambda_i X_c) \sin\left(\frac{\lambda_i W_s}{2}\right)}{\lambda_i} \varnothing(\lambda_i) + \frac{2}{k_{hs} W_{hs} L_{hs} L_s^2} \sum_{j=1}^{\infty} A_j \frac{\cos(\delta_j Y_c) \sin\left(\frac{\delta_j L_s}{2}\right)}{\delta_j} \varnothing(\delta_j) + \frac{4}{k_{hs} W_{hs} L_{hs} W_s^2 L_s^2} \sum_{i=1}^{\infty} \sum_{j=1}^{\infty} \times A_{ij} \frac{\cos(\lambda_i X_c) \sin\left(\frac{\lambda_i W_s}{2}\right) \cos(\delta_j Y_c) \sin\left(\frac{\delta_j L_s}{2}\right)}{\lambda_i \delta_j} \varphi(\beta_{ij}) \quad (5)$$

The parameters in (5) are defined in [11]. Equations (6, 7) define some constants to use in further relations; aspect ratio of microchannel (α), ratio of fin width to channel width (β), fin efficiency (η) and flow Reynolds number (Re) are given respectively.

$$\alpha = \frac{L_{ch}}{W_{ch}}, \beta = \frac{W_{fin}}{W_{ch}}, \eta = \frac{\tanh(m\alpha)}{m\alpha}, Re = \frac{\rho_f u_m D_h}{\mu_f} \quad (6)$$

$$m = \sqrt{Nu \frac{1 + \alpha}{\alpha \beta} \frac{k_f}{k_{hs}}}, u_m = \frac{V_f}{NW_{ch} L_{ch}}, D_h = \frac{2W_{ch} L_{ch}}{W_{ch} + L_{ch}} \quad (7)$$

Equation (8) presents the number of microchannels required for the heat sink.

$$N = \frac{W_{hs} - W_{fin}}{W_{ch} + W_{fin}} \quad (8)$$

Equation (9) presents the friction factor relation [10].

$$f \cdot R = 4.7 + 19.64G \quad (9)$$

Where,

$$G = \frac{\alpha^{-2} + 1}{(\alpha^{-1} + 1)^2} \quad (10)$$

Equation (11) defines the pressure drop across microchannel heat sink.

$$\Delta P = \frac{\rho_f u_m^2}{2} \left(4f \frac{L_{hs}}{D_h} + K \right) \quad (11)$$

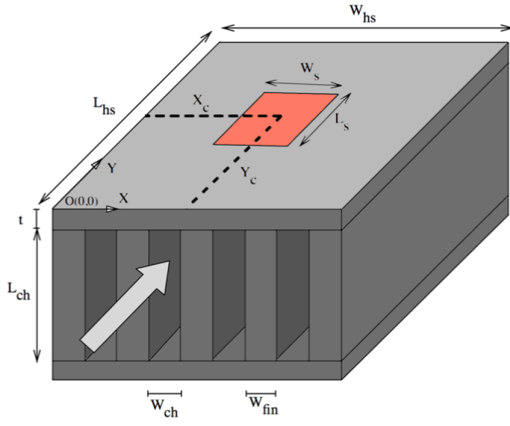


Figure 1. Schematic of microchannel heat sink and heat source

Where, loss coefficient (K) is given by [11].

$$K = 0.6\sigma^2 - 2.4\sigma + 1.8 \quad (12)$$

Where,

$$\sigma = \frac{NW_{ch}L_{ch}}{(W_{ch}L_{ch})} = \frac{NW_{ch}}{W_{hs}} \quad (13)$$

Equation (14) presents the nusselt number in the microchannel [11].

$$Nu = 8.235 \times \left(1 - \frac{2.042}{\alpha} + \frac{3.0853}{\alpha^2} - \frac{2.4765}{\alpha^3} + \frac{1.0578}{\alpha^4} - \frac{0.1861}{\alpha^5} \right) \quad (14)$$

III. METHODOLOGY

A. Multi-objective optimization algorithm

Most engineering problems are formulated as multiple objective functions which are mostly conflicted with each other. A typical deterministic constrained multi-objective optimization problem can be formulated as follows:

$$\begin{aligned} &\text{Find the vector } X = \{x_1, x_2, \dots, x_k\} \\ &\text{To minimize } f_i(x), \quad i = 1, 2, \dots, n \\ &\text{Subjected to } g_j(x) \leq 0, \quad j = 1, 2, \dots, m \end{aligned} \quad (15)$$

Where n is the number of objective functions, m is the number of constraints and $x \in R^k (x^L \leq x \leq x^U)$ is design variable vector with k elements.

B. Multi-objective Differential Evolution algorithm

Differential evolution is a strategy from evolutionary algorithms which is extensively used for global optimization problems since it was introduced. In this paper, a multi-objective uniform-diversity differential evolution algorithm which is recently proposed, adopted to solve the multi-objective constrained problem. The complete description of the algorithm can be found in [9].

C. Multi-objective design problem

The multi-objective design problem of a microchannel heat sink is given by:

$$\text{Min}_x \{R_{tot}, \Delta P\} \quad (16)$$

Subjected to:

$$Y_c < L_{hs} - \left(\frac{L_s}{2} \right)$$

$$X_c < W_{hs} - \left(\frac{W_s}{2} \right)$$

$$Y_c > \frac{L_s}{2}$$

$$W_c > \frac{W_s}{2}$$

$$5mm < L_{hs} < 15mm$$

$$5mm < W_{hs} < 15mm$$

$$30\mu m < L_{ch} < 300\mu m$$

$$30\mu m < W_{ch} < 300\mu m$$

$$30\mu m < W_{fin} < 300\mu m$$

$$2.5mm < X_c < 12.5mm$$

$$2.5mm < Y_c < 12.5mm$$

$$0.1mm < t < 3mm$$

This optimization problem included eight design variables and four geometric constraints to minimize two objective functions. Design variables consist of geometric parameters of the microchannel heat sink: L_{hs} , W_{hs} , L_{ch} , W_{ch} , W_{fin} , X_c , Y_c and t which are length of microchannel heat sink, width of microchannel heatsink, length of microchannel, width of microchannel, width of fin, centroidal X-coordinate and Y-coordinate of heat source and thickness of base of heat sink, respectively. Two objective functions considered for this problem: total thermal resistance and pressure drop. Both should be minimized; if total thermal resistance is minimized, the heat transfer rate from heatsink is increased which results in making the semiconductor cooler. Lowering pressure drop means less energy consumption for the outer pumping loop.

The geometric constraints are selected in the manner to keep the semiconductor in the surface of the microchannel heat sink in both vertical and horizontal directions.

TABLE I. DIFFERENTIAL EVOLUTION PARAMETERS

Parameter	Value
Population Size	100
Generations number	200
F (mutant factor)	0.6
Probability of crossover	0.9
Probability of Mutation	0.1
Var	0.1
ϵ -elimination threshold value	0.01

Both objective functions conflict with each other, it means that trying to minimizing an objective leads to maximizing the other. Hence, it's essential to employ methods to find a trade-off in minimizing both objective functions. The differential evolution parameters are presented in Table I.

D. Stochastic robustness analysis

Let X be a random variable, then the common model for uncertainties in stochastic randomness is the probability density function (PDF), $f_X(x)$ or equivalently the cumulative distribution function (CDF), $F_X(x)$, where the subscript X refers to the random variable. This can be given by (17).

$$F_X(x) = \Pr(X \leq x) = \int_{-\infty}^x f_X(x) dx \quad (17)$$

Where $\Pr(\cdot)$ is the probability that an event ($X \leq x$) will occur. Some statistical moments such as the first and the second moment, generally known as mean value (also referred to as expected value) denoted by $\mu(X)$ and variance denoted by $\sigma^2(X)$ respectively, are the most important ones. In the case of discrete sampling these functions can be shown by (18) and (19).

$$\mu(X) \cong \frac{1}{N} \sum_{i=1}^N x_i \quad (18)$$

$$\sigma^2(X) = Var(X) \cong \frac{1}{N-1} \sum_{i=1}^N (x_i - \mu(x))^2 \quad (19)$$

Where x_i is the i^{th} sample and N is the total number of samples.

IV. DISCUSSION AND RESULTS

A. Model validation

The governing equations described in section II were solved analytically for mass flow rates of 1 to 8 mL/s. Fig. 2 validates our model in comparison with the previous study. It indicates that the simulated model is in good agreement with experiments. This figure shows variation of total thermal resistance and pressure drop for different flow rates of the coolant. The used parameters and properties for this simulation are given in Table II. The heat sink material is considered as silicon (Si) and the heat source footprint of 5 mm \times 5 mm is also considered.

TABLE II. PARAMETERS USED FOR VALIDATION SIMULATION

Parameter	Value
L_{hs}	10mm
W_{hs}	10mm
L_{ch}	300 μm
W_{ch}	300 μm
W_{fin}	100 μm
X_c	5mm
Y_c	5mm
k_{hs}	100W/(m.K)
t	1.25mm

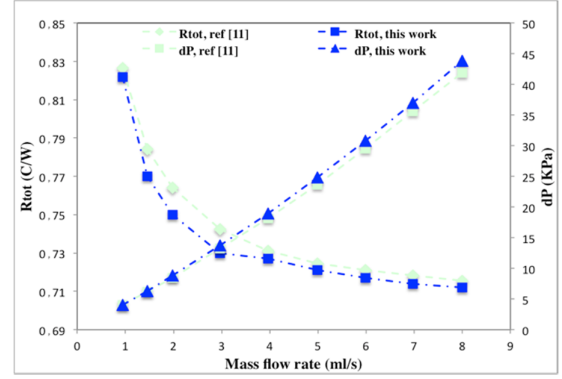


Figure 2. Variation of total thermal resistance and pressure drop along the microchannels for different mass flow rates of the coolant

B. Multi-objective optimization results

After 200 generations in a two-objective optimization process, all 100 initial individual in the population remained non-dominated with respect to each other. Fig. 3 depicts the ultimate non-dominated solutions of the optimization problem and the optimum design point A selected among them. To select the optimum point, the value of both objective functions for every ultimate solution in Pareto front mapped in the interval [0, 1] and summed their corresponding values. This method implies the normalized distance of the two objective functions.

$$F = \sqrt{f_1^2 + f_2^2} \quad (20)$$

C. Performance analysis of the optimum design point

The values of design variables and objective functions of the optimum design point (point A) are presented in Table III. The number of microchannels is obtained as 122 for optimum design point A based on (8). In addition the optimal location of the device obtained as 3.7mm along the x-axis and 2.7mm from the y-axis. Based on the optimum geometry of the heat sink $L_{hs}=5.4\text{mm}$ and $W_{hs}=7.3\text{mm}$, the heat source located near the center of the heat sink. Such location is analogous to the fact that, as the location of the device shifts from the inlet (or edge) toward the center (along the y-axis) of the heat sink, spreading resistance becomes the minimum and hence lowest total thermal resistance is achieved [11].

The plots of total thermal resistance and pressure drop based on the obtained optimal geometry are illustrated in Fig. 4. Total thermal resistance of the heat sink decreases from 0.913 to 0.753 $^{\circ}\text{C}/\text{W}$ and pressure drop increases from 0.824 to 2.551 kPa with flow rate variation from 0.5 to 1.5 mL/s. With increase in flow rate from 0.5 to 1.5 mL/s, decrease in total thermal resistance is 0.16 $^{\circ}\text{C}/\text{W}$ with an increase in pressure drop of 1.727 kPa. As suggested by [11], an optimum operating point can be where the curves for thermal resistance and pressure drop cross each other as evident in Fig. 4. This point corresponds to total thermal resistance of 0.782 $^{\circ}\text{C}/\text{W}$, 1.85 kPa of pressure drop and mass flow rate of 1.1 mL/s. While, the suggested optimum point by [11] (which can be seen from Fig. 1) corresponds to total thermal resistance of

0.738 °C/W, 15 kPa of pressure drop and the mass flow rate of 3.2 mL/s.

Hence, the prominent performance of the suggested geometry is obvious based on nominal variation between total thermal resistance of this study and of [11]. While, it consumes much less coolant and shows accordingly a significant optimality in pressure drop. It should be also noted that, the designers can choose another design point from the non-dominated solutions in Fig. 2 based on their priorities.

Fig. 5 shows that the temperature rise of coolant above the inlet temperature for optimum point abates when the mass flow rate increases; because more coolant is available to engross the dissipated heat from the heat source. Considering the optimum flow rate of 1.1 mL/s as previously discussed, the coolant will experience a temperature rise of 19.56 °C for a heat source dissipating 100W/cm².

D. Robustness analysis of the optimum design point

To evaluate the robustness performance of optimum design point to geometrical uncertainties, statistical analysis of this point is performed. Based on 5000 samples generated around the optimum point, the CDF plots of thermal resistance and pressure drop are depicted in Fig. 5. In this figure different uncertainty levels (3%, 5%, 7% and 10%) are assumed for robustness analysis.

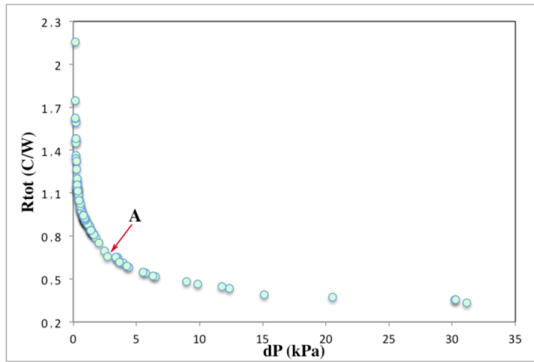


Figure 3. Pareto-front of non-dominated solutions of the optimization problem

TABLE III. DESIGN VARIABLES AND OBJECTIVE FUNCTIONS OF OPTIMUM DESIGN POINT A

Design variable	Optimum value
L_{hs} (mm)	5.4483
W_{hs} (mm)	7.3063
L_{ch} (μ m)	296.43
W_{ch} (μ m)	89.698
W_{fin} (μ m)	30.503
X_c (mm)	3.791
Y_c (mm)	2.782
t (mm)	0.3541
R_{tot} (C/W)	0.6574
dP (KPa)	2.7103

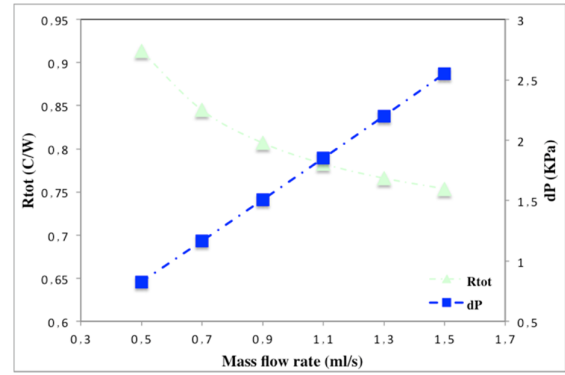


Figure 4. Variation of total thermal resistance and pressure drop for different mass flow rates of the coolant for optimum design point

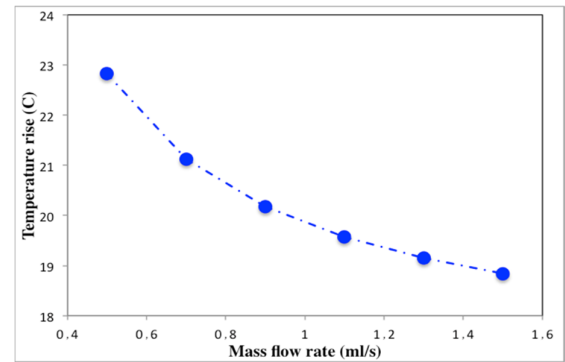


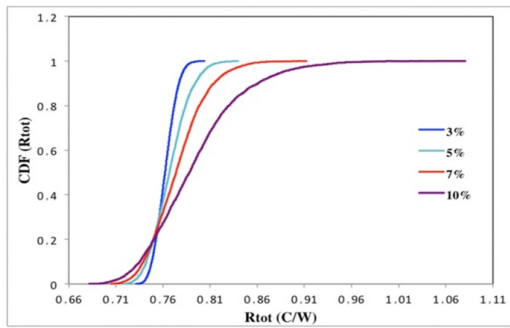
Figure 5. Temperature rise of microchannel heat sink for different mass flow rates for optimum design point

It can be seen from the Fig. 6 the suggested optimum point has relatively good robustness indices for less than 5% uncertainty level, which is the common uncertainty degree that suggested by many manufacturers. However, if the uncertainty level rises to more than 5% the suggested point is unreliable for practical purposes. In this case, the use of robust design procedure is crucial.

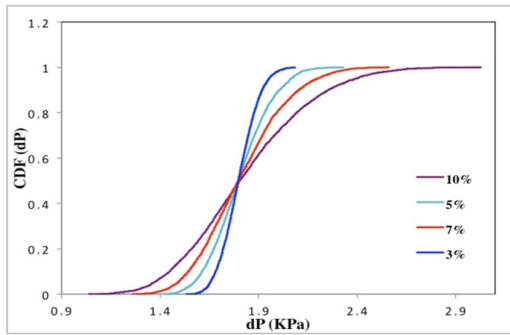
In addition to CDF plots, the PDF plots of the proposed optimum point demonstrated for the 5% uncertainty level in Fig. 7. The distribution of all samples from the mean values can be seen from these figures for both objective functions. Obviously, such distribution is more significant for higher uncertainty levels as can be seen from these figures.

V. CONCLUSION

This paper aimed to bridge the gap in multi-objective optimization studies of microchannel heat sink based on theoretical models and experimental correlations. In this way, a multi-objective differential evolution algorithm used for Pareto optimization of a single-phase liquid-cooled microchannel for microelectronics applications. Eight geometric parameters of the system considered as design variables. The total thermal resistance and pressure drop along the heat sink channels considered as objective functions. The optimum design point depicted from non-dominated solutions of multi-objective optimization.

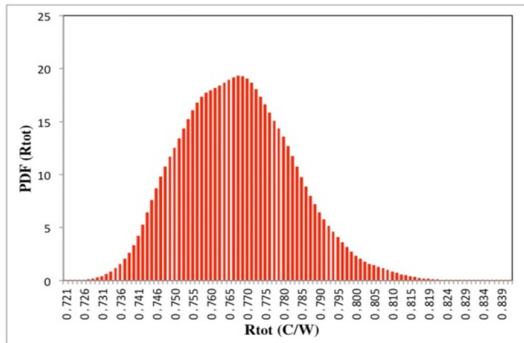


(a)

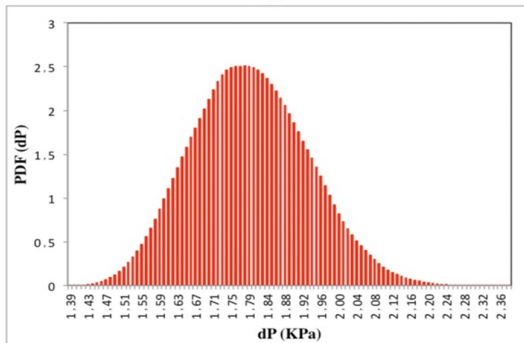


(b)

Figure 6. The Cumulative distribution function plot in optimum design point for different uncertainty levels



(a)



(b)

Figure 7. The probability density function plot both objective functions at 5% uncertainty level correspond to optimum design point A

The performance of the suggested optimum point showed for different mass flow rates. The results showed that solving the problem in a multi-objective fashion results in reaching an optimum point where lower pressure drop can be achieved in contrast with previous studies. In addition, a robustness analysis of the proposed geometry performed by using Monte Carlo Simulations. The simulations showed that the suggested design point has acceptable robustness level for 5% uncertainty in design variables and hence is reliable for practical purposes.

REFERENCES

- [1] Perret, Corinne, Jumana Boussef, Christian Schaeffer, and Martin Coyaud. "Analytic modeling, optimization, and realization of cooling devices in silicon technology." *Components and Packaging Technologies, IEEE Transactions on* 23, no. 4 (2000): 665-672.
- [2] Husain, Afzal, and Kwang-Yong Kim. "Shape optimization of micro-channel heat sink for micro-electronic cooling." *Components and Packaging Technologies, IEEE Transactions on* 31, no. 2 (2008): 322-330.
- [3] Kandlikar, Satish G. "History, advances, and challenges in liquid flow and flow boiling heat transfer in microchannels: a critical review." *Journal of Heat Transfer* 134, no. 3 (2012): 034001.
- [4] Dixit, Tisha, and Indranil Ghosh. "Review of micro-and mini-channel heat sinks and heat exchangers for single phase fluids." *Renewable and Sustainable Energy Reviews* 41 (2015): 1298-1311.
- [5] Ansari, Danish, Afzal Husain, and Kwang-Yong Kim. "Multiobjective optimization of a grooved micro-channel heat sink." *Components and Packaging Technologies, IEEE Transactions on* 33, no. 4 (2010): 767-776.
- [6] Storn, Rainer, and Kenneth Price. "Differential evolution—a simple and efficient heuristic for global optimization over continuous spaces." *Journal of global optimization* 11, no. 4 (1997): 341-359.
- [7] Sarangi, Suchismita, Karthik K. Bodla, Suresh V. Garimella, and Jayathi Y. Murthy. "Manifold microchannel heat sink design using optimization under uncertainty." *International Journal of Heat and Mass Transfer* 69 (2014): 92-105.
- [8] Bodla, Karthik K., Jayathi Y. Murthy, and Suresh V. Garimella. "Optimization under uncertainty applied to heat sink design." *Journal of Heat Transfer* 135, no. 1 (2013): 011012.
- [9] Gholaminezhad, I., and A. Jamali. "A multi-objective differential evolution approach based on ϵ -elimination uniform-diversity for mechanism design." *Structural and Multidisciplinary Optimization* (2015): 1-17.
- [10] Knight, Roy W., Donald J. Hall, John S. Goodling, and Richard C. Jaeger. "Heat sink optimization with application to microchannels." *Components, Hybrids, and Manufacturing Technology, IEEE Transactions on* 15, no. 5 (1992): 832-842.
- [11] Biswal, Laxmidhar, Suman Chakraborty, and S. K. Som. "Design and optimization of single-phase liquid cooled microchannel heat sink." *Components and Packaging Technologies, IEEE Transactions on* 32, no. 4 (2009): 876-886.